

Physics

Electricity & Magnetism fields

Okayama University

Year 1985

Finite element analysis of magnetic
circuits composed of axisymmetric and
rectangular regions

Takayoshi Nakata* N. Takahashi† Y. Kawase‡
H. Funakoshi** S. Ito††

*Okayama University

†Okayama University

‡Okayama University

**Okayama University

††Fukiage Factory, Fuji Electric Company Limited

This paper is posted at eScholarship@OUDIR : Okayama University Digital Information Repository.

http://escholarship.lib.okayama-u.ac.jp/electricity_and_magnetism/67

FINITE ELEMENT ANALYSIS OF MAGNETIC CIRCUITS COMPOSED OF AXISYMMETRIC AND RECTANGULAR REGIONS

T.Nakata, N.Takahashi, Y.Kawase, H.Funakoshi and S.Ito*

ABSTRACT

A new approximate method is developed for calculating three-dimensional magnetic fields in magnetic circuits composed of connected axisymmetric and rectangular regions. Using this new method, fairly accurate solutions can be obtained when the leakage flux from the magnetic circuit is small.

In this paper, the new method is explained and then the usefulness of the technique is clarified by comparing calculated and measured flux densities.

1. INTRODUCTION

Magnetic circuits are often composed of regions of axisymmetric shape and others of rectangular shape. Though three-dimensional analysis is required for such magnetic circuits, the magnetic fields have often been analyzed by the axisymmetric or the two-dimensional method to reduce computer storage and computing time.

A more accurate approximate method for analyzing such magnetic circuits has been developed by modifying and combining the axisymmetric and the two-dimensional finite element methods.

2. METHOD OF ANALYSIS

In this Section, first the new method is outlined. Next, a new vector potential is introduced in order to satisfy the continuity of flux on the boundary between the axisymmetric and the rectangular regions. Finally, the condition for the continuity of flux is derived, and the Rayleigh-Ritz equations are given.

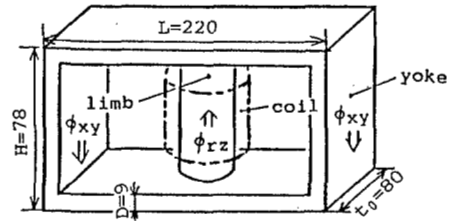
2.1 Outline of the Method

The new method can be illustrated by an example shown in Fig.1. Figure 1(a) shows the magnetic circuit, composed of a limb with circular section and a yoke with rectangular section. A coil is wound around the limb. Figure 1(b) shows the cross-section of the region to be analyzed.

Our method is derived by combining and modifying the usual axisymmetric and the two-dimensional finite element methods, in order to calculate three-dimensional magnetic fields within almost the same computing time and program size as the two-dimensional or the axisymmetric finite element method. An axisymmetric finite element method is applied to the region a-b-c-d-a, where the flux distribution is assumed to be axisymmetric, and a two-dimensional finite element method is applied to the region d-c-e-f-d, where the flux distribution is assumed to be two-dimensional. If both methods are simply combined, the flux is not always continuous on the boundary between two regions. A new vector potential is introduced to satisfy the condition of continuity of flux. If the leakage flux from the magnetic circuit is small due to the high permeability of the steel, fairly accurate solutions can be obtained by the new method.

The authors are with the Department of Electrical Engineering, Okayama University, Okayama 700, Japan.

The author* is with the Fukiage Factory, Fuji Electric Company Limited, Saitama 369-01, Japan.



(a) shape of model

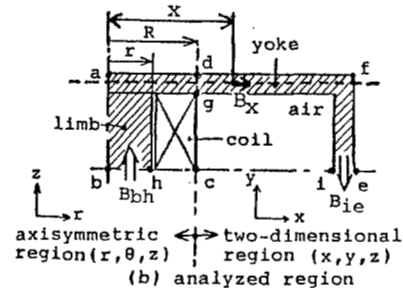


Fig.1 Analyzed model.

2.2 Introduction of New Vector Potential

If the vector potential on the boundary b-a-f-e in Fig.1(b) is assumed to be zero, the vector potential A_R defined by the following equation corresponds to the flux per radian in the limb [1].

$$A_R = r A_\theta, \tag{1}$$

where A_θ is the circumferential component of the vector potential in the axisymmetric field and r is the radius. The total flux ϕ_{rz} within the radius R in the limb can be written, using the vector potential A_R , by the following equation [1],

$$\phi_{rz} = 2\pi A_R, \tag{2}$$

The vector potential A_z in the two-dimensional field corresponds to the flux in the yoke per unit length in the z -direction. The total flux ϕ_{xy} in the yoke can be written, using the vector potential A_z , by

$$\phi_{xy} = t_0 A_z, \tag{3}$$

where t_0 is the thickness of the yoke. The following relationship between ϕ_{rz} and ϕ_{xy} can be obtained from the continuity of flux,

$$\phi_{rz} / 2 = \phi_{xy}. \tag{4}$$

By substituting (2) and (3) into (4), the following equation can be obtained,

$$\pi A_R = t_0 A_z. \tag{5}$$

When A_R and A_z are used for the analysis of the respective regions, A_R should be equal to A_z on the boundary. However, Eq.(5) indicates that the continuity of flux cannot be satisfied, when A_R is set to be equal to A_z .

Therefore, a new vector potential A which corresponds to the flux in a thickness t in the z -direction, is introduced in the rectangular region[2]. A is defined by the equation,

$$B_x = \frac{1}{t} \frac{\partial A}{\partial y}, \quad B_y = -\frac{1}{t} \frac{\partial A}{\partial x}, \tag{6}$$

where B_x and B_y are the x - and y -components of the flux density in the rectangular region, respectively. The total flux ϕ_{xy} in the yoke can be written, using the new vector potential A , by

$$\phi_{xy} = A t_0 / t. \tag{7}$$

From Eqs.(2), (4) and (7), the following relationship is obtained:

$$\pi A_R = A t_0 / t. \tag{8}$$

As A_R and A denote the fluxes in adjoining magnetic regions, A_R and A should be equal on the boundary $g-d$ between the two regions. Therefore, the thickness t which satisfies the continuity of flux can be derived from (8) as follows:

$$t = t_0 / \pi. \tag{9}$$

From Eqs.(7) and (9), ϕ_{xy} is finally written as

$$\phi_{xy} = \pi A. \tag{10}$$

Continuity of flux is also assumed on the boundary $c-g$ in the air. A_R and A are equal on the boundary $c-g$.

2.3 Formulations

Poisson's equation for the axisymmetric magnetic field can be written as follows [1]:

$$\frac{\partial}{\partial r} \left(\nu \frac{\partial A_R}{\partial r} \right) + \frac{\partial}{\partial z} \left(\nu \frac{\partial A_R}{\partial z} \right) = -J_{\theta\theta}, \tag{11}$$

where ν and $J_{\theta\theta}$ denote the reluctivity and the circumferential component of the current density, respectively.

Using the new vector potential A , Poisson's equation for the two-dimensional magnetic field can be written as follows:

$$\frac{\partial}{\partial x} \left(\nu \frac{\partial A}{\partial x} \right) + \frac{\partial}{\partial y} \left(\nu \frac{\partial A}{\partial y} \right) = -J_{\theta z}, \tag{12}$$

where, $J_{\theta z}$ is the z -component of the current density.

2.4 Rayleigh-Ritz Equations

The Rayleigh-Ritz equations can be obtained by minimizing the total energy X as follows:

$$\frac{\partial X}{\partial A_i} = 0 \quad (i=1, \dots, n), \tag{13}$$

where A_i is the vector potential at node i , and n is the number of nodes at which the vector potentials are unknown. A_i corresponds to A_R in the axisymmetric region and to A in the rectangular region. X is given by

$$X = X_{rz} + X_{xy}. \tag{14}$$

X_{rz} is the energy corresponding to Eq.(11) and is given by

$$X_{rz} = 2\pi \iint_{S_{rz}} \left(\frac{1}{2} \int_0^{B_{rz}^2} \nu dB_{rz}^2 - J_{\theta\theta} \frac{A_R}{r} \right) r dr dz, \tag{15}$$

where S_{rz} denotes the axisymmetric region.

X_{xy} is the energy corresponding to Eq.(12), in which the thickness t is replaced by Eq.(9), and is given by

$$X_{xy} = 2t_0 \iint_{S_{xy}} \left(\frac{1}{2} \int_0^{B_{xy}^2} \nu dB_{xy}^2 - \frac{\pi}{t_0} J_{\theta z} A \right) dx dy, \tag{16}$$

where S_{xy} denotes the rectangular region. The flux densities B_{rz} and B_{xy} in the respective regions can be represented by

$$B_{rz}^2 = \left(-\frac{1}{r} \frac{\partial A_R}{\partial z} \right)^2 + \left(\frac{1}{r} \frac{\partial A_R}{\partial r} \right)^2, \tag{17}$$

$$B_{xy}^2 = \left(\frac{\pi}{t_0} \frac{\partial A}{\partial y} \right)^2 + \left(-\frac{\pi}{t_0} \frac{\partial A}{\partial x} \right)^2. \tag{18}$$

3. FACTORS AFFECTING THE ACCURACY

The effects of the position of the boundary between the axisymmetric and the rectangular regions, and the shape of the magnetic circuit on the accuracy of the calculated results are investigated.

3.1 Position of the boundary

The flux distribution in the magnetic circuit shown in Fig.1 has been analyzed. The radius of the limb and radius of the coil are 19 and 39(mm), respectively. The thickness of the yoke is 80(mm). The boundary positions investigated are denoted by the broken lines in Fig.2.

Figure 3 shows the effects of the position R of the boundary on the average flux densities B_{bh} and B_{ie} of the limb and the yoke denoted in Fig.2. The ampere turn $I \times n$ of the coil is 0.25x850 and 1x850(AT). The solid lines denote the calculated results and the broken lines denote the measured ones. The shape of the yoke inside the boundary is different from the true one. As the percentage of such a part of the yoke is small compared with the total magnetic circuit, the accuracies of B_{bh} and B_{ie} are not affected much by the position R .

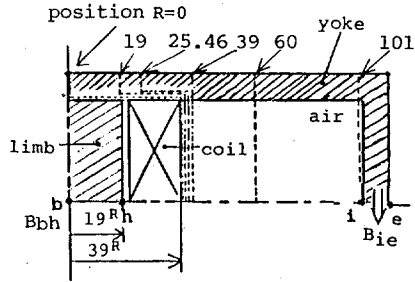


Fig.2 Position of the boundary.

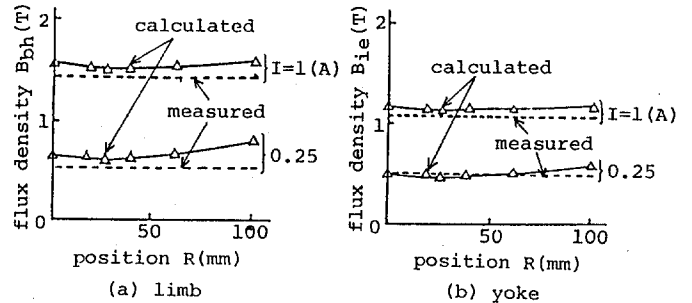


Fig.3 Effects of the position of the boundary on the flux densities.

Figure 4 shows the x -component B_x of the flux density at the point which is x (mm) from the center line as denoted in Fig.1(b). B_x is increased with x during $x < 16$ (mm). When $x \geq 16$ (mm), the increase of the cross-sectional area becomes larger than that of the amount of the flux. Therefore, B_x has the peak value near $x = 16$ (mm). In this model, the cross-sectional areas of the axisymmetric and rectangular regions on the boundary are equal to each other when R is 25.46(mm). The assumed sections of the limb at the positions $R = 19, 25.46, 60$ (mm), for examples, are shown in Fig.5. Although the continuity of the flux at the boundary is considered as denoted in 2.2, the flux density B_x is not continuous at the boundary when R is not equal to 25.46(mm) as shown in Fig.4. Therefore, the boundary should be set on the position where respective cross-sectional areas of the boundaries of both regions are the same.

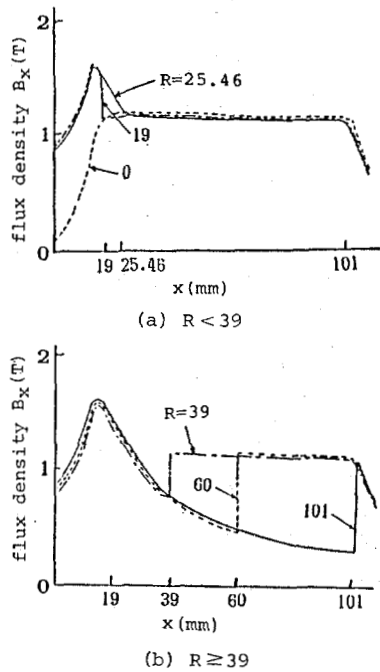


Fig. 4 Effects of the position R on the flux distribution.

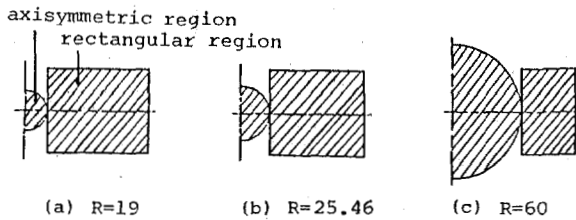


Fig. 5 Assumed sections of the axisymmetric and rectangular regions at each position of the boundary.

3.2 Shape of the magnetic circuit

The dimension of the magnetic circuit shown in Fig. 1 is determined by the radius r of the limb, and the length L , the width D , the thickness t_0 and the height H of the yoke. When, the conventional two-dimensional method is applied to the whole region, the error due to the radius of the limb is considerable, because the whole region is assumed to be rectangular. If the magnetic field of this magnetic circuit is analyzed using the axisymmetric or the two-dimensional method, there are some errors in the calculated flux densities because such a method assumes that the whole region is axisymmetric or rectangular. The error of the cross-sectional area of the yoke is mainly due to the radius r of the limb, and the length L and the thickness t_0 of the yoke. Therefore, the effects of r , L and t_0 on the flux densities B_{bh} and B_{ie} are analyzed. The current in the coil is 1(A), and the boundary is at $R=25.46$ (mm).

Figures 6, 7 and 8 show the effects of the radius r of the limb and the length L and the thickness t_0 of the yoke on B_{bh} and B_{ie} . Results using the new method are denoted by " Δ ". " \circ " and " \times " denote flux densities calculated using the axisymmetric and the two-dimensional method, respectively. Experimental results are denoted by " \square ". The results calculated using the new method show good agreement with the experimental ones for almost every r , L and t_0 . The results calculated using the axisymmetric and the two-dimensional methods, however, are very much

different from the experimental ones. This is because the new method can take account of the cross-sectional areas of the limb and the yoke.

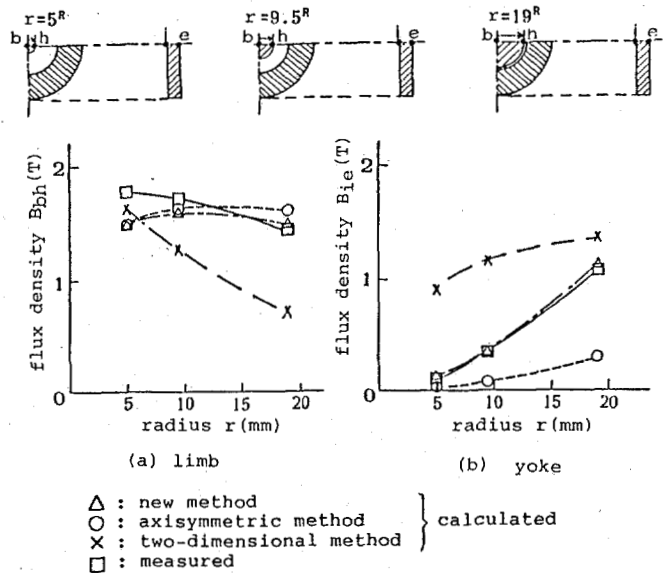


Fig. 6 Effects of the radius r of the limb on the flux densities ($I=1A$).

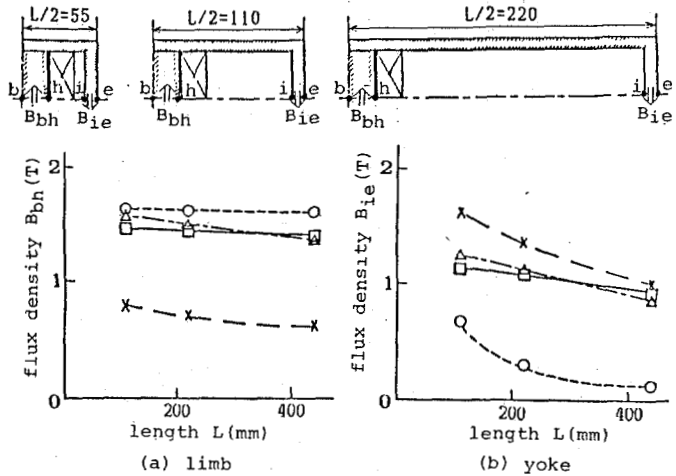


Fig. 7 Effects of the length L of the yoke on the flux densities ($I=1A$).

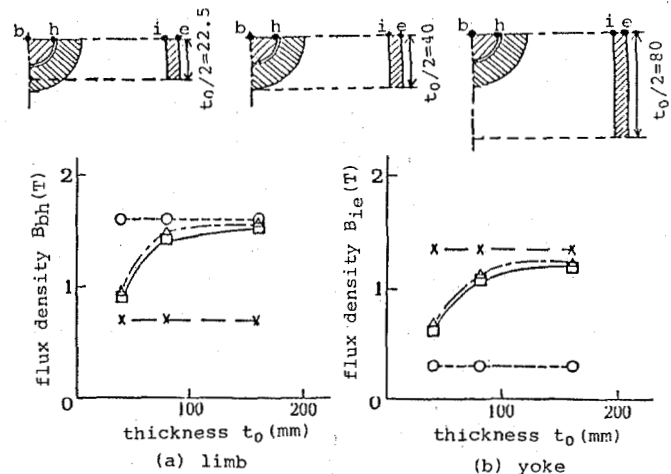


Fig. 8 Effects of the thickness t_0 of the yoke on the flux densities ($I=1A$).

4. APPLICATION TO A MAGNETIZER

Figure 9 shows one quadrant of an analyzed magnetizer. The permanent magnet to be magnetized is set between the two pole pieces. The pole piece and the yoke are made of steel. The number of turns of the coil is 840.

The axisymmetric finite element method is applied to the region b-a-f-e-d-c-b, and the two-dimensional finite element method is applied to the region c-d-e-f-g-h-c. The boundary e-f is chosen as the position where the cross-sectional areas of the boundaries of the axisymmetric and the rectangular regions are the same.

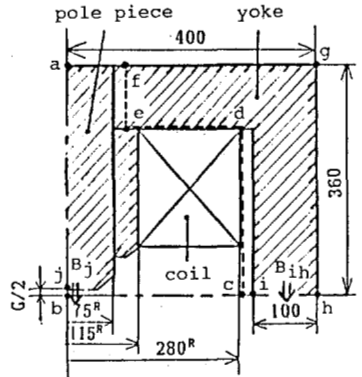
Figure 10 shows the flux distributions. The solid line denotes the flux line in the axisymmetric region and the broken line in the rectangular region.

Figure 11 shows the calculated and the measured flux densities. B_j and B_{ih} denote the flux density at the point j and the average flux density on the line i-h in Fig.9. As the leakage flux is distributed axisymmetrically, the results calculated using the new method show good agreement with the experimental ones.

5. CONCLUSIONS

The new method enables us to analyze magnetic circuits composed of connected axisymmetric and rectangular regions requiring only a small increase of computer storage and computing time. The accuracy of the method depends on the position of the boundary between the two regions, the permeability, etc. A more detailed investigation of the accuracy will be reported later.

It is also possible to analyze the flux distributions in magnetic circuits composed of more than two kinds of rectangular regions with different thickness [4]. The method will be improved so that magnetic circuits with more than two kinds of axisymmetric regions can be analyzed.



Boundary conditions
 b-a-g-h: Dirichlet boundary
 b-h : Neumann boundary

Fig.9 Model of a magnetizer.

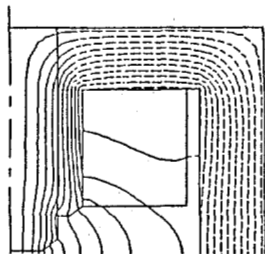
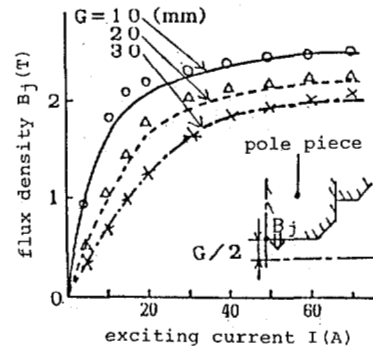
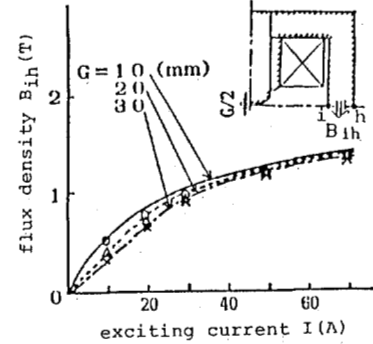


Fig.10 Flux distribution
 (I=20A, G=10mm).



(a) flux density B_j at the pole tip



(b) flux density B_{ih}

— } calculated O } measured
 - - - } Δ }
 - · - } X }

Fig.11 Excitation characteristics.

REFERENCES

- [1] T.Nakata and N.Takahashi: "Finite Element Method in Electrical Engineering" (book, in Japanese), Morikita Shuppan, Tokyo, 1982.
- [2] T.Nakata et al: "Interdisciplinary Finite Element Analysis" (book), Cornell University, Ithaca, 1981.
- [3] T.Nakata, Y.Kawase, H.Funakoshi and S.Ito: "Finite Element Analysis of a Magnetic Circuit Composed of Axisymmetric and Cartesian Coordinates", Papers of Combined Technical Meeting on Rotating Machines and Static Apparatus, RM-83-39, SA-83-29, IEE, Japan, 1983.
- [4] T.Nakata, Y.Kawase, H.Funakoshi and S.Ito: "Improvement of the Hybrid Finite Element Method and its Application", Papers of Combined Technical Meeting on Rotating Machines and Static Apparatus, RM-84-22, SA-84-6, IEE, Japan, 1984.